chemengineering

MDPI

Brief Report

Chemical Species Formed on FeB-Fe_2B Layers during Wet Sliding Wear Test

Ricardo Andrés García-León * and Nelson Afanador-García

Grupo de Investigación INGAP & CERG, Facultad de Ingeniería, Universidad Francisco de Paula Santander Ocaña, Ocaña C.P. 546552, Colombia; nafanadorg@ufpso.edu.co

* Correspondence: ragarcial@ufpso.edu.co; Tel.: +57-3152898250

Abstract: In the present work, X-ray photoelectron spectroscopy (XPS) survey spectra of borided AISI 316L for two different times (1 and 6 h) of exposure to simulated body fluid (SBF) were obtained after wet sliding wear. A borided layer of ~39 microns was obtained on the surface of the AISI 316L stainless steel using the thermochemical treatment of boriding. As part of the mechanical and chemical characterization of sliding wear, Berkovich nanoindentation and X-ray spectroscopy tests were used to determine the main properties of the borided layer. The results of the specific wear rate values were higher at 5 mm/s sliding speed than those recorded at 30 mm/s due to the influence of the exposure time of the sample and the complex combinations of chemical reactions with boron (e.g., B_2S_3, Cr_2O_3, and Fe_2O_3) on the surface during the sliding during 6 h of exposure in Hank's solution due to the formation of the passive film. The knowledge of chemical species formed during wet sliding wear tests on borided AISI 316L is essential for understanding wear mechanisms and materials' performance and optimizing material properties and materials' and components' reliability in the biomedical industry for screws and fastening plates.

Keywords: wear; lubrication; chemical species; mechanical contact

Citation: García-León, R.A.; Afanador-García, N. Chemical Species Formed on FeB-Fe_2B Layers during Wet Sliding Wear Test. *ChemEngineering* **2024**, *8*, 22. https://doi.org/10.3390/chemengineering8010022

Academic Editor: Ewa Kowalska

Received: 17 September 2023
Revised: 16 October 2023
Accepted: 31 October 2023
Published: 9 February 2024

1. Introduction

AISI 316L alloy has found applications in the field of medicine owing to its favorable characteristics, including biocompatibility, chemical composition, and cost-effectiveness, particularly in the manufacturing of screws and fixation plates [1]. However, one of the notable drawbacks of AISI 316L alloy is its long-term performance, primarily due to its relatively low mechanical properties, such as wear and fatigue resistance [2]. Low wear properties mean that AISI 316L is less prone to material loss due to friction and abrasion (improved thermally or thermochemically). Low wear is beneficial in implants, such as joint replacements or orthopedic devices, because it reduces the likelihood of debris generation. Reduced wear can minimize the risk of adverse tissue reactions, implant loosening, and the need for revision surgeries. Implants are designed to have a long service life within the body. The low wear properties of AISI 316L contribute to the longevity of the implant. However, low fatigue properties are essential for implants subjected to cyclic loading, such as joint prostheses. These implants must withstand repetitive stresses during activities like walking or joint movement. Low fatigue properties ensure the implant's structural integrity over time, reducing the risk of mechanical failure. Implant fractures can lead to severe complications and may require surgical interventions. Also, minimizing the risk of fatigue-related fractures in load-bearing implants provides greater safety and reliability [3]. These limitations and characteristics can be addressed by modifying the material's surface by applying different thermal or thermochemical treatments, which, when combined with the base material, create thin layers/coatings. These modifications enhance its tribological performance by reducing surface damage in different environments.

The powder pack boriding process (PPBP) represents a surface thermochemical treatment (boron diffusion) that enhances various industrial materials' hardness, wear resistance,

and corrosion resistance. PPBP offers several advantages over other thermo-chemical processes. It operates at lower temperatures, reducing distortion and preserving material properties. PPBP enhances surface hardness, provides thickness control, and ensures good adhesion and uniformity. It is environmentally friendly, versatile, and can be tailored to specific applications. Short processing times and reduced energy consumption make it a cost-effective choice for surface modification [4].

Ceramic coatings exhibit responses to conventional lubricants like those exhibited by metals; it is important to note that while there are commonalities in the response of ceramics and metals to conventional lubricants, there are also significant differences. Ceramics often have unique properties, including high hardness, wear resistance, and low thermal expansion, which can affect their tribological behavior differently from metals. The choice of lubricant and the design of the tribological system should consider the specific characteristics and requirements of the materials involved. In this way, adequate lubrication reduces the incidence of asperity contact, diminishes surface shear stresses, and lowers material removal. However, it is worth noting that even under lubricated conditions, chemical interactions can still play a significant role in the industry [5].

Several studies have explored the behavior of borided AISI 316L in simulated body fluid environments without considering the effect of sliding speed during wear. For instance, Hanawa et al. [1] researched the chemical characterization of oxide films developed on AISI 316L stainless steel in various simulated body fluid environments, employing the XPS technique to identify the resulting chemical reactions. Campos-Silva et al. [6] assessed the tribocorrosion resistance and cytotoxicity of borided AISI 316L, utilizing a ball-on-flat configuration and Hank's solution. They adhered to the ASTM G119-09 standard [7] procedure to calculate wear–corrosion synergy. Mejía-Caballero et al. [8] evaluated the corrosion resistance of borided and non-borided AISI 316L over ten days using SBF (Hank's solution). Meanwhile, Kayali et al. [9] investigated the corrosion behavior of borided AISI 316L samples using electrochemical methods in an SBF solution and employed a ball-on-disc configuration for their experiments.

Contribution of This Work

In this study, the effect of the sliding speed on the passive film formed on borided AISI 316L stainless steel after a wet sliding wear test immersed in Hank's solution was characterized using XPS to estimate the chemical species formed on the surface, considering a previous work [10]. The knowledge of chemical species formed during wet sliding wear tests on borided AISI 316L is essential for understanding wear mechanisms, assessing materials' performance, optimizing material properties, and ensuring the reliability of materials and components in real-world applications. It aids in material selection, design, and quality control, ultimately contributing to enhanced performance and durability.

This work provides valuable insights into the effects of boriding treatment on the wear resistance and surface properties of AISI 316L stainless steel in an SBF environment. The findings have implications for improving the durability and performance of materials used in biomedical and engineering applications, where wear and corrosion resistance are crucial factors. Additionally, this study highlights the importance of considering exposure time and chemical reactions in understanding material behavior in challenging environmental conditions.

2. Materials and Methods

2.1. Boriding Thermochemical or Powder Pack Boriding Process

Commercial samples of AISI 316L stainless steel, with a nominal chemical composition in weight percent (17.56 Cr, 10.75 Ni, 2.11 Mo, 1.40 Mn, 0.51 Si, 0.03 P, 0.02 S, 0.02 C, and 67.59 Fe), were obtained as determined in [11]. AISI 316L samples were cut into discs measuring 20 mm in diameter and 4 mm in thickness. The profilometry analysis using Bruker Contour equipment confirmed that the surface roughness of overall analyzed

samples of AISI 316L was Ra $\leq$ 0.05 µm. The AISI 316L stainless steel samples exhibited a surface hardness (H) of around 2.10 GPa and a Young's modulus (E) of around 242 GPa.

PPBP was conducted at a temperature of 1223 K for a duration of 4 h to develop a borided layer with a thickness of around 30 µm (considering the kinetic model proposed by [12]) using a powder mixture composed of SiC, B_4C, and KBF_4 (activator, donator, and diffuser) enclosed in a cylindrical case, without the use of an inert atmosphere. After completing the PPBP, the container was extracted from the furnace and gradually cooled to room temperature. Note that for specific applications in the biomedical industry, the short processing times and reduced energy consumption of PPBP make it a cost-effective choice for surface modification.

2.2. Mechanical and Chemical Characterizations

A mirror-finished sample of borided AISI 316L with metallographic preparation was used to identify the growth on the cross-section of the FeB and Fe_2B layers using SEM/JEOL equipment operating at 20 kV. The Berkovich nanoindentation test using a CSM instrument applying a constant load of 100 mN was used to determine the H and E behavior.

Wet sliding wear tests of the borided AISI 316L samples were performed using the UMT-2/Bruker tribotest based on the ASTM G133-05 standard [13] procedure with a ball-on-flat condition using an alumina ball of 6 mm in diameter. With the aim of evaluating the behavior of the SBF solution (used as a lubricant with similar properties to the blot [14]), the following test parameters were a total sliding distance (D) of 100 m, two different sliding speeds (5 and 30 mm/s = 6 and 1 h of time exposure), stroke length of 10 mm, and a constant load (L) of 10 N.

After the wet sliding wear tests, the wear volume removed material (V) was measured across the wear tracks by optical profilometry using Bruker Contour equipment, and the specific wear rate (k) was estimated with the equation proposed by Archard, $k = V(L \times D)$—(mm^3/Nm) [15].

Finally, XPS analysis of the wear center surface composition of the borided AISI 316L steel was performed using a Thermo Scientific K-Alpha, equipped with a monochromatic AlK-α X-ray source with an energy level of 1487 eV and featuring a dual-mode flood source for compensating charges (DMFG).

3. Results and Discussion

3.1. Chemical Microstructure of the Borided AISI 316L Steel

The total layer thickness composed of FeB and Fe_2B is ~39 µm, with FeB = 30.41 $\pm$ 2.0 µm and Fe_2B = 8.55 $\pm$ 0.6 µm, as shown in Figure 1. The flatness of the borided layer on the AISI 316L steel can be attributed to the presence of alloying elements that impede its expansion. It has been documented that chromium (Cr), nickel (Ni), and molybdenum (Mo) serve as diffusion barriers at the boundary between the borided layer and the substrate, in addition to a decreased concentration of carbon, silicon, and boron [16–24]. In addition, each chemical element contributes to the layer growth restriction; Cr is a key element in stainless steel alloys, including AISI 316L, known for its corrosion resistance properties, and it forms a protective passive oxide layer on the surface of the steel, which acts as a barrier to prevent further corrosion.

In the same way, Ni, another important alloying element in AISI 316L stainless steel, enhances the steel's corrosion resistance, particularly in aggressive environments; like Cr, Ni contributes to forming a protective passive film on the steel's surface. This passive film, often composed of nickel oxide (NiO), serves as a barrier to boron diffusion, restricting the borided layer's growth. Finally, Mo is added to stainless steel to improve its resistance to pitting and crevice corrosion, especially in chloride-containing environments, which also can form protective oxides (e.g., molybdenum oxide, MoO_3) on the steel's surface, which enhances the material's overall corrosion resistance. Similar to chromium and nickel, the presence of molybdenum-based oxides creates a diffusion barrier for boron, limiting its penetration and the growth of the borided layer. Finally, these oxide layers act as barriers

that impede boron diffusion into the material. As a result, the thickness and growth of the borided layer are limited, impacting the effectiveness of boriding treatments on this specific type of stainless steel [19].

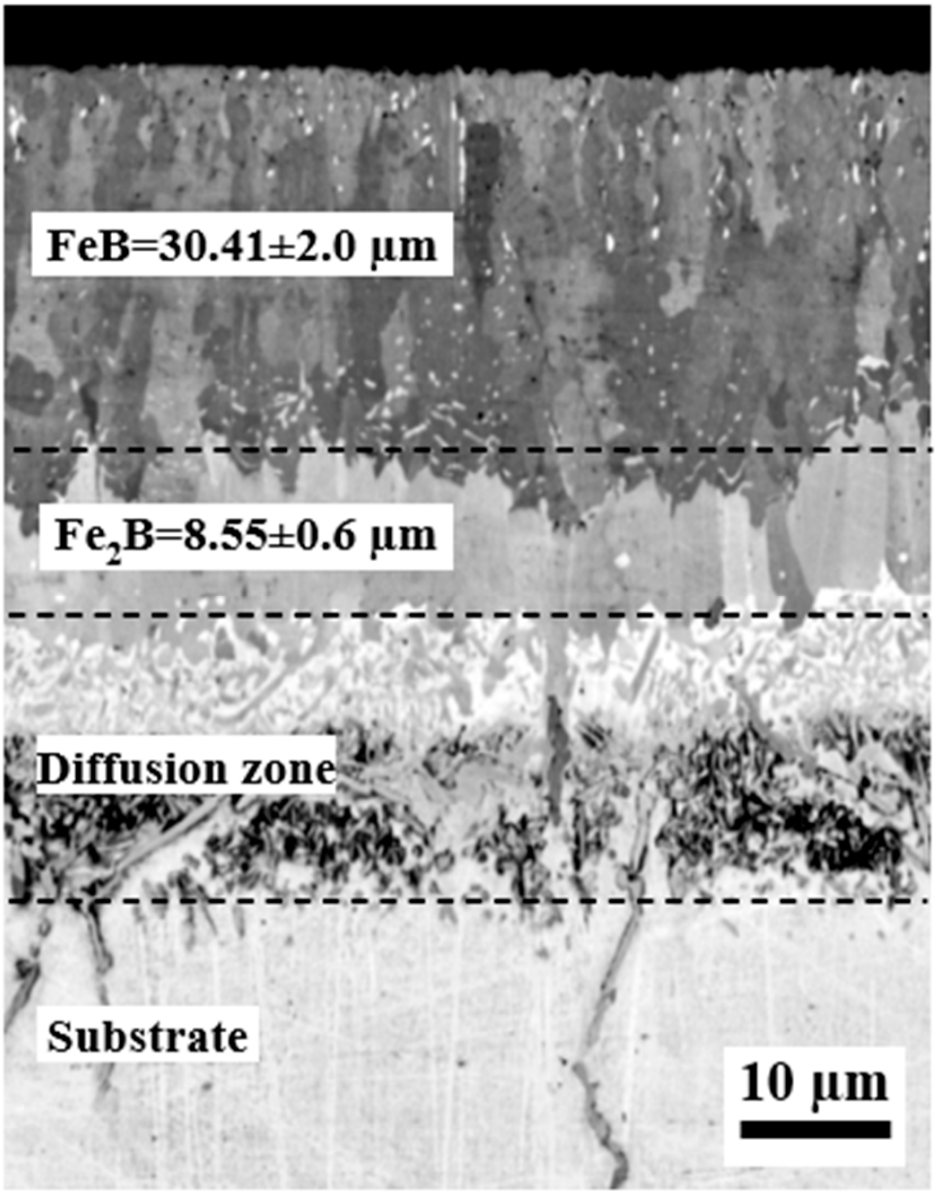

Figure 1. Microstructure of the borided AISI 316L by SEM.

3.2. Instrumented Nanoindentation Berkovich Test Results

The nanoindentation distances on the borided layer were measured using an Olympus/GX51 metallurgical microscope and Image-Pro Plus software. The hardness (H) and Young's modulus (E) profile are shown in Figure 2. The behavior of H and E values was measured in the ranges of 23–21 GPa and 381–358 GPa (for FeB) and 18–17 GPa and 340–331 GPa (for Fe_2B), until a value of around ~3.5 GPa with 235 GPa in the substrate was measured, respectively. The E values are directly related to the trace size effect obtained during the sensed nanoindentation test to measure the material elasticity, as was observed [20,21], and similar results were reported in [20,22].

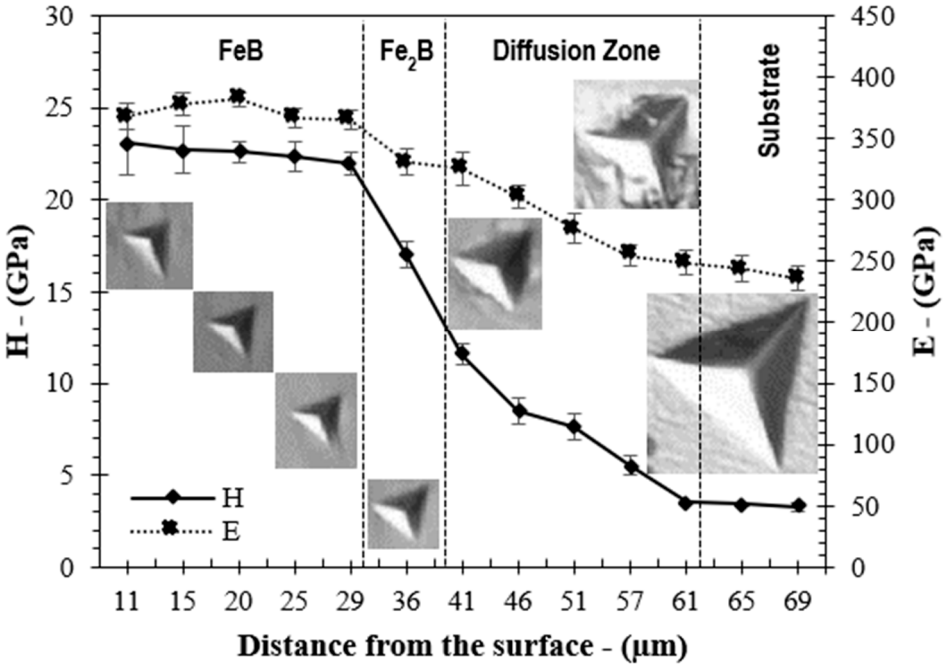

Figure 2. Behavior of hardness (H) and Young modulus (E) in cross-section.

3.3. Sliding Wear Behavior of the Borided AISI 316L Stainless Steel

Sliding wear revealed the behavior of the friction coefficient (CoF) concerning the relative wear sliding distance for the iron boride layer of the borided AISI 316L when subjected to an Al_2O_3 ball under wet conditions. The borided AISI 316L samples revealed CoF values of around 0.28 and 0.20 for exposure times of 6 and 1 h, respectively. However, for non-borided AISI 316L samples, the highest CoF values obtained were around 0.45 and 0.29 for 6 and 1 h exposure times, respectively, as reported in [10]. Fluctuations/changes in the CoF behavior could be attributed to various wear mechanisms, the layer's anisotropy, and the occurrence of the stick–slip phenomenon, which led to the entrapment and expulsion of wear particles (a three-body mechanism), and related to the extent of material transfer from the surface to the counterpart [23].

Lubricants, such as Hank's solution, create a thin film on contacting surfaces, preventing direct contact and influencing friction and wear characteristics. In the literature, one or more SBF lubricants (salt solutions) have been employed to assess the wear properties of implant materials [24]. However, it is worth noting that Hank's solution did not produce a sufficiently thick lubrication film, resulting in CoF values ranging between 0.3 and 0.5 [25]. Adequate lubrication reduced the occurrence of asperity contact, minimized surface shear stresses, and reduced material removal. In the experimental conditions examined, Hank's solution led to a boundary lubrication regime ($\lambda \leq 1$). Nevertheless, even under lubricated conditions, chemical effects remained significant [5].

Specific wear rates were obtained with the equation proposed by Archard in a wet medium (Hank's solution), showing average values 3.6 times lower for the borided AISI 316L samples (4.77–2.91 $\times$ 10^{-6} mm^3/Nm considering exposure times of 6 and 1 h, for borided AISI 316L) than for non-borided AISI 316L steel (17.74–9.66 $\times$ 10^{-6} mm^3/Nm considering exposure times of 6 and 1 h). For the same wear conditions in dry tests, *k* for the non-borided AISI 316L steel was 224–447.4 $\times$ 10^{-6} mm^3/Nm and 5.3–8.9 $\times$ 10^{-6} mm^3/Nm for the borided AISI 316L steel [26]; the borided steel *k* value was on average 45 times lower than that of the non-borided AISI 316L steel [27]. This behavior has been previously reported by Kayali [9]. Also, as reported in [28,29], and [30], for ceramics, the specific wear rate does not necessarily decrease with the use of lubricants and can even increase. Comparing results from this study and those reported by [23,26], borided AISI 316L steel *k* values in a wet medium are ~2 times lower than those in a dry medium, while AISI 316L

steel *k* values in a wet medium are ~22 lower than those in a dry one. In wet conditions, debris acts as an abrasive that ruptures the hydrodynamic film in a lubricating system due to the real contact pressure on each asperity contact.

The boundary lubrication regime does not fully cover the surface roughness (even with low Ra values), where roughness during sliding wear supports most of the load (contact pressure), generating micro-welding, plastic deformation (wear track edge), and the direct interaction between the tribopairs Al_2O_3/borided AISI 316L. Note that high contact pressures and low sliding speeds are typical in this lubrication regime, influenced by the low viscosity of the lubricant (Hank's solution). Considering the above, the scheme shown in Figure 3 is established, showing that under the boundary lubrication regime and the action of sliding wear, the influence of the type of elastohydrodynamic lubrication of the particles of Hank's solution is generated [31].

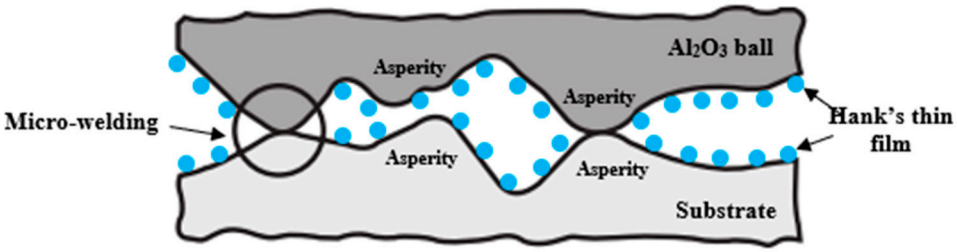

Figure 3. Schematic representation of the boundary lubrication regime.

The surface oxidation during sliding is increased by the action of the temperature that might increase when the sliding speed increases too (facilitating the oxidation of the sliding surfaces aided by the lubricant). This behavior can reduce the wear rate by transforming the wear metallic particles into wear oxide particles (tribo-oxidative wear mode) [32]. Tribo-oxidative wear mode can occur at low sliding speeds with the evidence of the oxide wear particles on the surface-worn track. The decrease in the specific wear rate with increased sliding speed for borided AISI 316L steel has previously been attributed to accelerated stress corrosion due to frictional heating (triggering oxidation due to low sliding speed related to the exposure time) [33]—the formation of an oxide layer that protects the surface against wear being complex to determine.

In metals such as Fe, Ni, Co, and Mo, the oxide film on the surface forms and grows as a crystalline film. However, in the case of Al, Si, and Cr, the oxidation has a light reaction from amorphous layers, and then these layers are transferred to the tribopairs [32]. This hard coating mainly develops the abrasive and adhesive wear mode because of the contact pressure between tribopairs (borided AISI 316L/Al_2O_3 ball), which is 1.89 GPa calculated from Hertzian theories. At some points, adhered material removal, passive film in Cr_2O_3, Fe_2O_3, or B_2O_3 chemical products, or both phenomena appear. Around the worn Al_2O_3 balls, smearing should be observed due to the action of the debris that interacted with Hank's solution, which generated dark areas that are more evident depending on the exposure time, as was previously reported by [10].

3.4. XPS Analysis after Wet Wear Test on the Borided AISI 316L Stainless Steel

The chemical compositions of the borided AISI 316L steel after 1 and 6 h of wear tests in Hank's solution were analyzed employing the XPS technique, as shown in Figure 4. The survey spectrum of borided AISI 316L stainless steel after the immersion in Hank's solution evidenced the presence of chemical elements such as B, Ni, Cr, Fe, F, O, N, Ca, P, and Cl. B1s and O1s spectra were examined to identify the species formed over the surface of the borided AISI 316L.

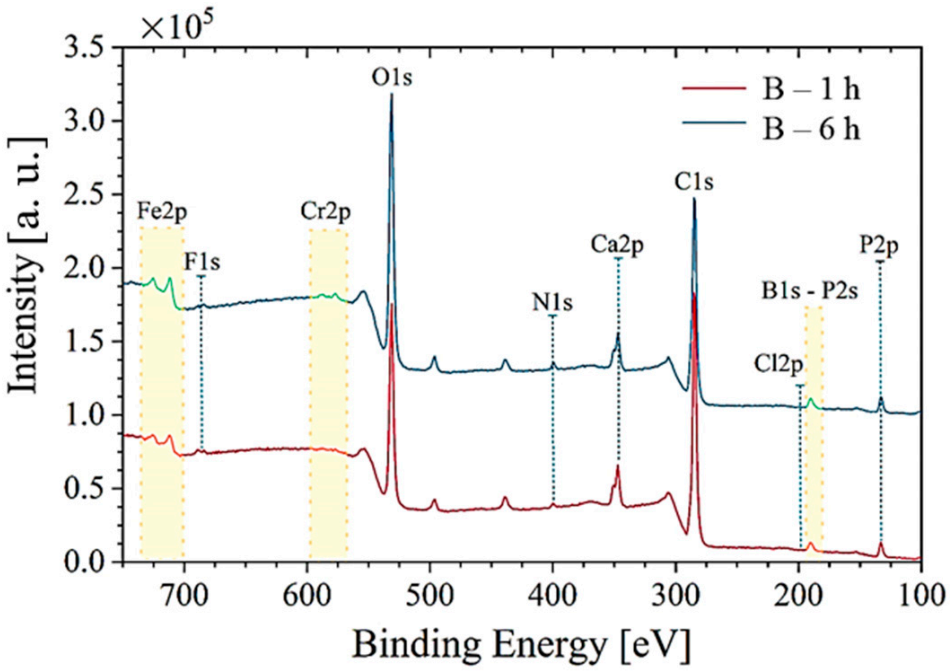

Figure 4. XPS survey spectra of borided AISI 316L for two different exposure times. Note: Red line is for 1 h, and blue line is for 6 h of exposition.

The chemical species contents in atomic percentage obtained from analysis of XPS spectra are reported in Figures 5 and 6 for both exposure times (1 and 6 h). The content of the B element in the borided AISI 316L steel increased from 6.1 to 6.9 wt%. According to [34], the boride values decreased to 0.9 wt. % after the 5th day of immersion in Hank's solution, affecting the borided layer corrosion resistance due to the low level of boron compounds acquired during the boriding process. Notice that the chemical species contributions related to each peak are named as they appear in the high-resolution spectra (i.e., B_1, B_2, B_3, B_4, and B_5 are related to borided AISI 316L steel, P is related to both samples, and the Cl change of chemical species is related to the material). The levels of B_2S_3, $FePO_4$ chemical species, and boron compounds (FeB, Fe_2B, CrB, Cr_2B, Ni_2B, and Ni_3B) present are similar to those reported by [6]. These elements change the morphology and chemical composition of the borided AISI 316L steel surface, affecting the wear and corrosion behavior.

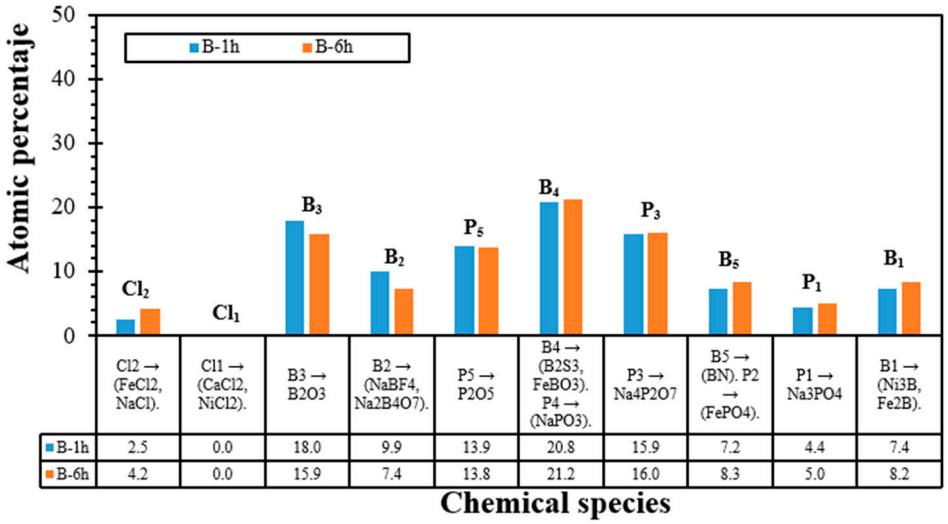

Figure 5. Cl2p-P2s-B1s chemical species determined by XPS analysis on the borided AISI 316L surface.

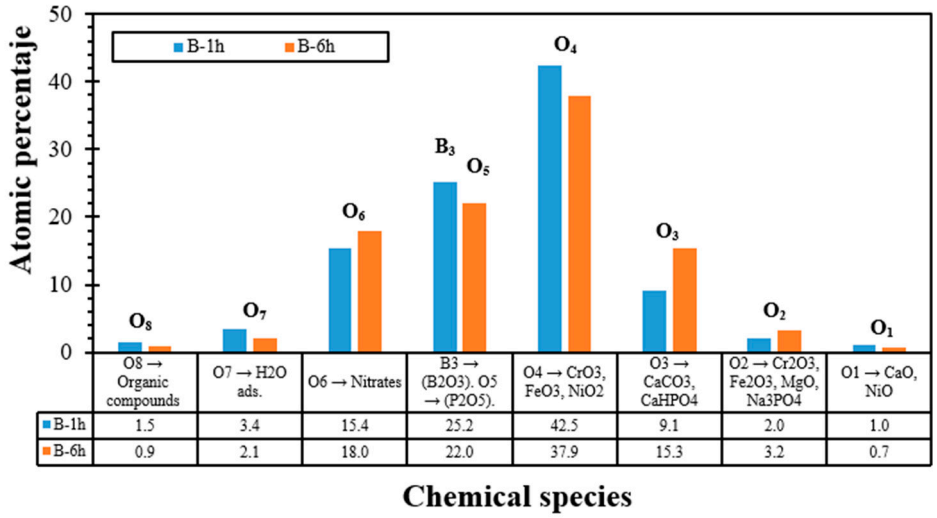

Figure 6. O1s chemical species determined by XPS analysis on the borided AISI 316L surface.

On the other hand, the Cl ions form dissolvable complex salts (e.g., $CrCl_3$, $FeCl_2$, and $NiCl_2$) with alloying elements of the AISI 316L stainless steel. During sliding wear, the formation of dissolvable complex salts, such as $CrCl_3$, $FeCl_2$, and $NiCl_2$, with alloying elements in AISI 316L stainless steel can occur due to several factors: (1) When the stainless steel surface is exposed to a corrosive environment such as one containing chloride ions (Cl^-), chemical reactions can take place between the alloying elements (e.g., chromium, iron, and nickel) and the chloride ions, forming complex chloride salts. (2) Chloride ions can react with metal cations, such as Cr^{3+}, Fe^{2+}, and Ni^{2+}, present in stainless steels. These reactions form soluble chloride complexes, where the chloride ions bind with metal cations to create stable, soluble compounds. (3) The specific conditions during sliding wear, including the presence of moisture, temperature, and mechanical stress, can promote these chemical reactions; little local frictional heating and mechanical forces can enhance the dissolution of metal ions and their interaction with chloride ions. (4) While some corrosion processes can lead to the degradation of materials, in certain cases, they can also form protective oxide or chloride layers on the surface, which can act as a barrier, preventing further corrosion or wear. (5) The composition of borided AISI 316L stainless steel, which includes alloying elements like chromium, iron, and nickel, makes it susceptible to specific chemical interactions with chloride ions, forming complex salts.

The passive film formed on the surface of the borided AISI 316L steel is made up of a complex combination of chemical interactions between boron, sulfate, and phosphate carrier species (B_2O_3, H_2BO_3, B_2S_3, and $Na_2B_4O_7$), which leads to the development of pits and cracks on the surface (see Figure 7). On the other hand, cracks are probably caused by galvanic coupling resulting from the difference in electrochemical properties at the coating/substrate interface, characteristic of corrosion mechanisms. According to [6], Hank's solution increases the corrosion resistance for 72 h, and the passive film acts as protection against wear due to minimizing the contact between tribopairs (Al_2O_3/surface) [15], thus reducing wear; after this period, the passive film is dissolved (with a tendency for partial dissolution due to the electrolyte), and the corrosion resistance and wear decrease. The passive film on the borided AISI 316L steel is composed of elements such as Fe_2O_3, MgO, P_2O_5, B_2O_3, metal hydroxides, organic compounds, carbonates, and phosphates [35]. On many occasions, the growth of the passive films is influenced by mechanical wear during sliding under tribocorrosion tests [6]. The passivation increase of i_{corr} = 0.21 μA/cm^2 and i_{corr} = 0.71 μA/cm^2 for borided AISI 316L stainless steel was reported by Campos-Silva et al. [6]. Also, the presence of SO_4^{2-} and PO_4^{2+} in Hank's solution promotes the accumulation of reaction products as B_2S_3 and $FePO_4$ [8]. However, borided AISI 316L steel exhibits increased corrosion speed due to the surface's pore amount related to the thermochemical treatment [9].

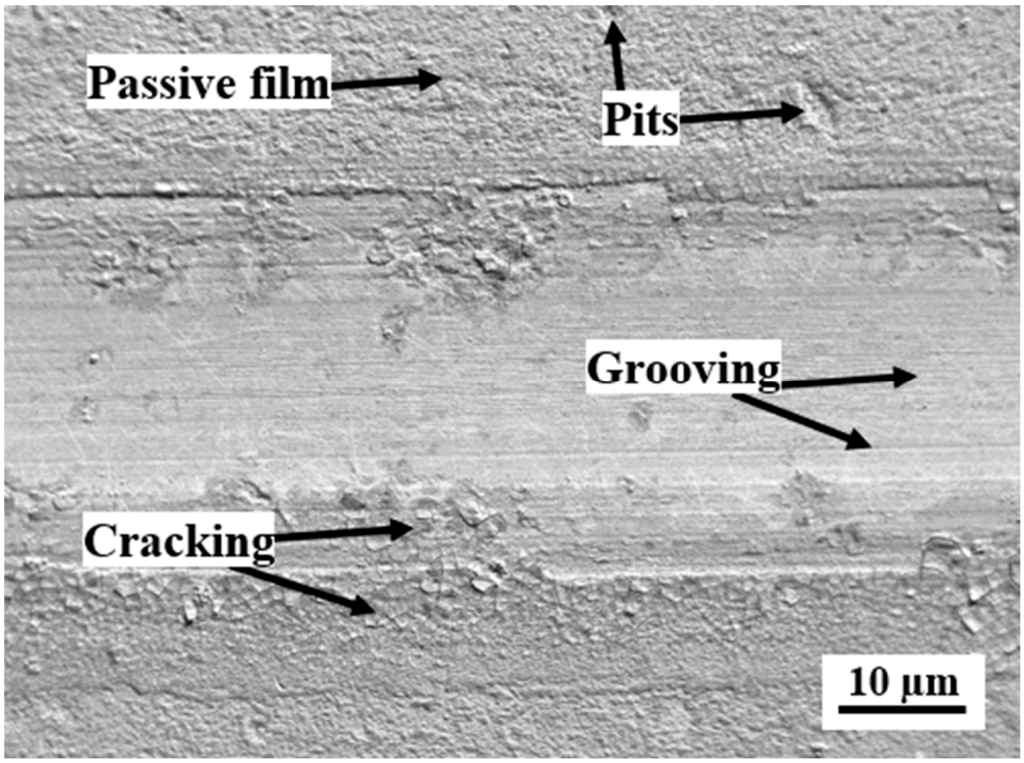

Figure 7. Main wear mechanisms over the surface.

During the reciprocating sliding wear, the passive film was formed and destroyed in each pass and fell off the Al_2O_3 ball, which was affected by the time of the frequency of sliding (repassivation process) [6]. However, the Al_2O_3 counterpart passes over the surface, where the wear particles are exposed to Hank's solution, while the counterpart removes the passive film, thus forming it on the opposite side as it passes the surface (>0.25 cycles/s takes time to form). On the other hand, the contact points change continuously due to the wear action, which is related to oscillations of the CoF during sliding and, thus, the formation of the densest passive film where no mechanical contact is generated.

The environment composition can cause the FeB-Fe_2B layer to passivate and become soluble or insoluble corrosion products (chemical species), forming a mixed layer of wear products and their interaction with Hank's solution, which aids in reducing material removal volume, specific wear rate, and CoF. This passive film decreases CoF, the wear volume, and the specific wear rate; this performance could be evidenced in the CoF behavior [36].

3.5. Human Body Implant Effects

In real conditions, the corrosion products on borided AISI 316L steel implanted in the femur as a part of an artificial hip joint consist of chromium combined with sulfur and/or iron and phosphorus-containing calcium and chlorides. Iron is preferentially released, and chromium is concentrated on the surface in a chloride solution. In this process, the iron is freely released. According to Hanawa et al. [1], a passive film in a real implant in the human body is not always macroscopically stable and does not ensure excellent tribological performance. Also, concerning chemical products on the implant, the passive film is formed mainly of calcium and phosphorus on stainless steel.

The cytotoxicity study of Campos-Silva et al. [6] revealed that borided AISI 316L steel provides satisfactory properties for the survival and proliferative activity of human fibroblasts and Vero cells on the surface for biomedical applications, with the presence of boron compounds (FeB, Fe_2B, CrB, Cr_2B, and Ni_2B) and various types of salts ($CaCl_2$, NaCl, $NaHCO_3$, and KCl from the culture medium). A thin layer of H_2BO_3 on the surface of

borided AISI 316L steel was found to be biocompatible with MDCK cells when cytotoxicity was tested in vitro, with a protective effect against cellular stress, according to [37]. In addition, low CoF and good biocompatibility evidence that this borided material might be used for joint prostheses under constant wear. On the other hand, chemical species such as BPO_4 positively affect cellular viability in in vitro and in vivo studies.

The effect of iron boride toxicity, focusing on FeB and Fe_2B layers immersed in SBF, is significant in various industrial and biomedical applications. Iron borides are commonly employed for surface modification and coating of materials, offering enhanced wear resistance and durability. However, understanding the potential toxicity of these borides is crucial, especially when they are used in contexts involving exposure to biological environments. This paper elaborates on the impact of iron boride toxicity in immersion scenarios. In the biomedical field, the biocompatibility of borided layers plays a pivotal role. FeB and Fe_2B layers are generally considered biocompatible, making them suitable for applications like medical implants and devices. Nevertheless, individual patient responses can vary, necessitating comprehensive biocompatibility assessments.

4. Conclusions

The specific wear rate was ~3.6 times lower for the borided AISI 316L samples than for non-borided AISI 316L steel. This behavior is explained by the formation of different oxides that could reduce the mechanical contact between the tribopairs (Al_2O_3/surface), thus reducing material removal.

The boundary lubrication regime ($\lambda \leq 1$) is related to low lubricant thickness, which was found for the sliding contact between the tribopairs of Al_2O_3 and borided AISI 316L steels immersed in Hank's solution, promoting material removal.

After wet sliding wear tests, the FeB phase disappeared from the surface because of the formation of the B_2S_3 species on the surface of the borided AISI 316L steel, promoting an increase in this chemical species when the exposure time increased during the sliding wet wear test; maybe these species protect the surface against wear. In addition, the formation of B_2S_3 species is indicative of a chemical reaction between boron and sulfur in the corrosive environment.

The corrosion and wear resistance of borided AISI 316L steels is related to corrosion products such as B_2S_3 and Fe_2O_3 formed during the sliding wear test; these corrosion products interact with Hank's solution and the surfaces affecting the performance of the steels.

The simulated body fluid formed chemical reactions that form corrosion products, both soluble and insoluble, forming a mixed layer with the wear products that aid in reducing the volume, material removal, wear rate, and CoF on the surface of the borided AISI 316L steels. During wear generated in the linear reciprocating wear test, oxide islands/points are generated by sliding contact, tribo-chemical reactions between tribopairs, and low velocities and reduce material transfer to the opposite surface and, therefore, material volume removal.

Author Contributions: R.A.G.-L., contributed to investigation, conceptualization, methodology, formal analysis, funding acquisition, original draft, writing—review and editing, other contributions. N.A.-G., methodology, funding acquisition, other contributions. All authors have read and agreed to the published version of the manuscript.

Funding: This work was supported by the research grant 158-08-037 of the Universidad Francisco de Paula Santander Ocaña.

Data Availability Statement: No data were used for the research described in the article.

Acknowledgments: R.A.G.-L. thanks the IPN and the DIE of the UFPSO for their support in the postdoctoral stance, and financial resources for this work (CVU-745458).

Conflicts of Interest: The authors declare that they have no known competing financial interests or personal relationships that could have appeared to influence the work reported in this paper.

References

1. Hanawa, T.; Hiromoto, S.; Yamamoto, A.; Kuroda, D.; Asami, K. XPS characterization of the surface oxide film of 316L stainless steel samples that were located in quasi-biological environments. *Mater. Trans.* **2002**, *43*, 3088–3092. [CrossRef]
2. Peruzzo, M.; Serafini, F.L.; Ordonez, M.F.C.; Souza, R.M.; Farias, M.C.M. Reciprocating sliding wear of the sintered 316L stainless steel with boron additions. *Wear* **2019**, *422–423*, 108–118. [CrossRef]
3. Davis, J.R. Mechanical Properties of Carbon and Alloy Steels. In *Metals Handbook Desk Edition*, 2nd ed.; CRC Press: Boca Raton, FL, USA, 1998.
4. García-León, R.A.; Martínez-Trinidad, J.; Campos-Silva, I. Historical Review on the Boriding Process using Bibliometric Analysis. *Trans. Indian Inst. Met.* **2021**, *74*, 541–557. [CrossRef]
5. Hutchings, I.; Shipway, P. *Sliding Wear*; Elsevier Ltd.: Amsterdam, The Netherlands, 2017.
6. Campos-Silva, I.; Palomar-Pardavé, M.; Pérez Pastén-Borja, R.; Kahvecioglu Feridun, O.; Bravo-Bárcenas, D.; López-García, C.; Reyes-Helguera, R. Tribocorrosion and cytotoxicity of FeB-Fe_2B layers on AISI 316 L steel. *Surf. Coat. Technol.* **2018**, *349*, 986–997. [CrossRef]
7. *ASTM-G119-09*; Guide for Determining Synergism between Wear and Corrosion. ASTM International: West Conshohocken, PA, USA, 2009.
8. Mejía-Caballero, I.; Palomar-Pardavé, M.; Martínez Trinidad, J.; Romero-Romo, M.; Pérez Pasten-Borja, R.; Lartundo-Rojas, L.; López-García, C.; Campos-Silva, I. Corrosion behavior of AISI 316L borided and non-borided steels immersed in a simulated body fluid solution. *Surf. Coat. Technol.* **2015**, *280*, 384–395. [CrossRef]
9. Kayali, Y.; Büyüksagis, A.; Yalcin, Y. Corrosion and Wear Behaviors of Boronized AISI 316L Stainless Steel. *Met. Mater. Int.* **2013**, *19*, 1053–1061. [CrossRef]
10. García-León, R.A.; Martínez-Trinidad, J.; Campos-Silva, I.; Figueroa-López, U.; Guevara-Morales, A. Development of tribological maps on borided AISI 316L stainless steel under ball-on-flat wet sliding conditions. *Tribol. Int.* **2021**, *163*, 107161. [CrossRef]
11. Acequisa 2018 Aceros y Equipos S.L. Aleación AISI 316L. Available online: https://acequisa.com/tipologia/inoxidables-especiales-austeniticos-y-superausteniticos/ (accessed on 23 August 2022).
12. Campos-Silva, I.; Ortiz-Domínguez, M.; Tapia-Quintero, C.; Rodríguez-Castro, G.; Jiménez-Reyes, M.Y.; Chávez-Gutiérrez, E. Kinetics and boron diffusion in the FeB/Fe_2B layers formed at the surface of borided high-alloy steel. *J. Mater. Eng. Perform.* **2012**, *21*, 1714–1723. [CrossRef]
13. *ASTM-G133-05*; Standard Test Method for Linearly Reciprocating Ball-on-Flat Sliding Wear. ASTM International: West Conshohocken, PA, USA, 2016.
14. Mejía-Caballero, I. *Evaluación de la Resistencia a la Corrosón en Aceros Aleados de Uso Industrial Endurecidos Por Difusión Superficial de Boro*; Instituto Politecnico Nacional: Mexico City, Mexico, 2011.
15. Holmberg, K.; Matthews, A. *Coatings Tribology: Properties, Mechanisms, Techniques and Applications in Surface Engineering*; Elsevier: Oxford, UK, 2009.
16. Özbek, I.; Konduk, B.A.; Bindal, C.; Ucisik, A.H. Characterization of borided AISI 316L stainless steel implant. *Vacuum* **2002**, *65*, 521–525. [CrossRef]
17. Jurči, P.; Hudáková, M. Diffusion Boronizing of H11 Hot Work Tool Steel. *J. Mater. Eng. Perform.* **2011**, *20*, 1180–1187. [CrossRef]
18. Kunst, H.; Schaaber, O. Beobachtungen beim Oberflächenborieren von Stahl II-Über Wachstumsmechanismen und Aufbau der bei der Eindiffusion von Bor in Eisen bei Gegenwart von Kohlenstoff entstehenden Verbindungs- und Diffusionsschichten. *Harterei-Tech. Mitt.* **1967**, *22*, 131–140.
19. García-León, R.A.; Afanador-García, N.; Guerrero-Gómez, G. A Scientometric Review on Tribocorrosion in Hard Coatings. *J. Bio-Tribo-Corrosion* **2023**, *9*, 39. [CrossRef]
20. García-Léon, R.A.; Martínez-Trinidad, J.; Campos-Silva, I.; Wong-Angel, W. Mechanical characterization of the AISI 316L alloy exposed to boriding process. *DYNA* **2020**, *87*, 34–41. [CrossRef]
21. Taktak, S. Some mechanical properties of borided AISI H13 and 304 steels. *Mater. Des.* **2007**, *28*, 1836–1843. [CrossRef]
22. Reséndiz-Calderon, C.D.; Rodríguez-Castro, G.A.; Meneses-Amador, A.; Campos-Silva, I.E.; Andraca-Adame, J.; Palomar-Pardavé, M.E.; Gallardo-Hernández, E.A. Micro-Abrasion Wear Resistance of Borided 316L Stainless Steel and AISI 1018 Steel. *J. Mater. Eng. Perform.* **2017**, *26*, 5599–5609. [CrossRef]
23. García-León, R.A.; Martinez-Trinidad, J.; Zepeda-Bautista, R.; Campos-Silva, I.; Guevara-Morales, A.; Martínez-Londoño, J.; Barbosa-Saldaña, J. Dry sliding wear test on borided AISI 316L stainless steel under ball-on-flat configuration: A statistical analysis. *Tribol. Int.* **2021**, *157*, 106885. [CrossRef]
24. Majumdar, P.; Singh, S.B.; Chakraborty, M. Wear properties of Ti–13Zr–13Nb (wt.%) near β titanium alloy containing 0.5wt.% boron in dry condition, Hank's solution and bovine serum. *Mater. Sci. Eng. C* **2010**, *30*, 1065–1075. [CrossRef]
25. Conradi, M.; Kocijan, A.; Klobčar, D.; Podgornik, B. Tribological response of laser-textured Ti6Al4V alloy under dry conditions and lubricated with Hank's solution. *Tribol. Int.* **2021**, *160*, 107049. [CrossRef]
26. García-León, R.A.; Martínez-Trinidad, J.; Campos-Silva, I.; Figueroa-López, U.; Guevara-Morales, A. Wear maps of borided AISI 316L steel under ball-on-flat dry sliding conditions. *Mater. Lett.* **2021**, *282*, 128842. [CrossRef]
27. García-León, R.A.; Martínez-Trinidad, J.; Guevara-Morales, A.; Campos-Silva, I.; Figueroa-López, U. Wear Maps and Statistical Approach of AISI 316L Alloy under Dry Sliding Conditions. *J. Mater. Eng. Perform.* **2021**, *30*, 6175–6190. [CrossRef]

28. Mischler, S.; Muñoz, A.I. Wear of CoCrMo alloys used in metal-on-metal hip joints: A tribocorrosion appraisal. *Wear* **2013**, *297*, 1081–1094. [CrossRef]
29. Rainforth, W.M. The wear behaviour of oxide ceramics—A Review. *J. Mater. Sci.* **2004**, *39*, 6705–6721. [CrossRef]
30. Hutchings, I.; Shipway, P. *Tribology: Friction and Wear of Engineering Materials*, 2nd ed.; Butterworth-Heinemann: Oxford, UK, 2017.
31. Blazquez de Mingo, A. Análisis de la Lubricación Termo-Elastohidrodinámica y Mixta Mediante la Aplicación de Modelos Numéricos (España). 2016. Available online: https://oa.upm.es/43073/1/TFG_ALVARO_LORENZO_BLAZQUEZ_DE_MINGO.pdf (accessed on 29 November 2022).
32. Menezes, P.; Ingole, S.; Nosonovsky, M.; Kailas, S.V.; Lovell, M.R. *Tribology for Scientists and Engineers*; Springer: New York, NY, USA, 2013.
33. Bhushan, B. *Modern Tribology Handbook Volume One*; CRC Press: Boca Raton, FL, USA, 2001.
34. Mejía-Caballero, I.; Escobar-Martínez, C.; Palomar-Pardavé, M.; Le Manh, T.; Romero-Romo, M.; Rodríguez-Clemente, E.; Lartundo-Rojas, L.; Campos-Silva, I. On the Corrosion Mechanism of Borided X12CrNiMoV12-3 Steel Immersed in a Neutral Aqueous Solution Containing Chloride and Sulfate Ions. *Metall. Mater. Trans. A Phys. Metall. Mater. Sci.* **2020**, *51*, 4868–4879. [CrossRef]
35. Yan, Y. *Bio-Tribocorrosion in Biomaterials and Medical Implants*; Elsevier: New York, NY, USA, 2013.
36. Kato, K.; Adachi, K. Wear of advanced ceramics. *Wear* **2002**, *253*, 1097–1104. [CrossRef]
37. Chino-Ulloa, A.; Hernandes-Alejandro, M.; Castrejón-Flores, J.L.; Cabrera-González, M.; Torres-Avila, I.P.; Velázquez, J.C.; Ruiz-Trabolsi, P.A.; Hernández-Sánchez, E. Development of ultra-low friction coefficient films and their effect on the biocompatibility of biomedical steel. *Mater. Trans.* **2019**, *60*, 1605–1613. [CrossRef]